Journal of Materials Chemistry A

Accepted Manuscript

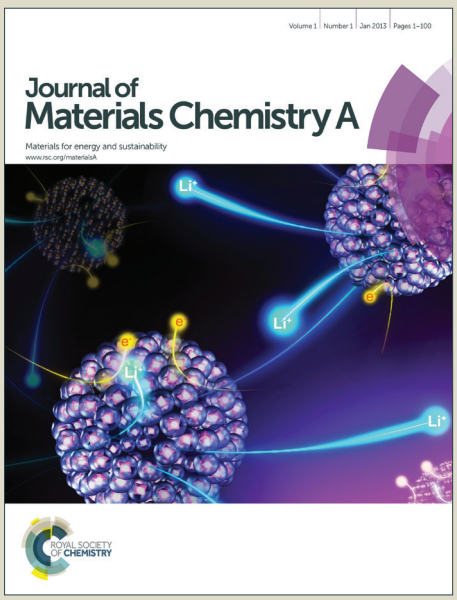

ROYAL SOCIETY OF CHEMISTRY

www.rsc.org/materialsA

High performance of Polyimide/ $CaCu_3Ti_4O_{12}$@Ag hybrid films with enhanced dielectric permittivity and low dielectric loss

Yang Yang[1], Haoliang Sun[1], Di Yin[1], Zhihong Lu[3], Jianhong Wei[1], Rui Xiong[1,5,*], Jing Shi[1], Ziyu Wang[1,2], Zhengyou Liu[1], Qingquan Lei[4]

[1]*Key Laboratory of Artificial Micro- and Nano-structures of Ministry of Education and School of Physics and Technology, Wuhan University, Wuhan 430072, P. R. China*

[2]*Dongfeng Commercial Vehicle Technology Center, Wuhan 430056, P. R. China*

[3]*School of Materials and Metallurgy, Wuhan University of Science and Technology, Wuhan 430081, P. R. China*

[4]*School of Electrical Engineering, Wuhan University, Wuhan 430072, P. R. China*

[5]*Hubei Collaborative Innovation Center for Advanced Organic Chemical Materials, Wuhan 430062, P. R.China*

*Corresponding author: Rui Xiong, Email: xiongrui@whu.edu.cn

This work reports the excellent dielectric properties of polyimide (PI) embedded with $CaCu_3Ti_4O_{12}$(CCTO)/Ag nanoparticles (CCTO@Ag). By functionalizing the surface of CCTO nanoparticles with Ag coating, the dielectric permittivity of PI/CCTO@Ag composites is significantly increased to 103 (100Hz) at 3 vol% filler loading. The enhancement of dielectric permittivity is attributed to the increment of conductivity of the interlayer between CCTO and PI by Ag, which enhances the space charge polarization and Maxwell-Wagner-Sillars (MWs) effect. The experimental results fit well with percolation theory. Moreover, the low loss (0.018 at 100Hz) is achieved attributed to blockage of charge transfer by insulating polyimide chains. It is shown that the electrical field distortion is significantly improved by decorating the surface of CCTO nanoparticles with Ag using Comsol Multiphysics. This plays an important role in the

enhancement of dielectric properties.

Introduction:

Novel materials for embedded passive applications are in great and urgent demand, in which polymer based materials with easy processibility and tunable property have been attractive. Especially, polymeric nanocomposites associated with high dielectric permittivity (high k), low dielectric loss and easy processibility have been in increasing demand in high charge-storage capacitors and high-speed integrated circuits[1-8]. Many efforts have been devoted to this research and the main methods are processing 'Two-phases' composites including ceramic ($Pb(Zr,Ti)O_3$(PZT) and $BaTiO_3$ (BT) et al.)/polymer and conductive fillers(silver, nickel et al.)/polymer composites [9-11]. The biggest problem is that the dielectric losses are always high due to the high content of ceramic and insulator-conductor transition for two kinds of composites, respectively[12-24]. So the main purpose is to substantially raise the dielectric permittivity of the composites while retaining low loss tangent. To do this, surfactant treatment of filler by coupling agent or by decorating insulating or conducting particles have become research focus recently[25]. It is proved that the fabrication of inorganic/metal structure will reduce the loss tangent while maintain improvement of the dielectric permittivity[21, 26-28]. The increment of conductivity of the interlayer between filler and polymer matrix by conducting particles promote the space charge polarization and polarization reverse speed, which will certainly enhance the dielectric permittivity and retain low loss tangent. $CaCu_3Ti_4O_{12}$ (CCTO) has attracted much attention for its high dielectric permittivity over a wide temperature range from 100K to 500K [29,30]. The giant high dielectric permittivity of CCTO will make great contribution to the increment of composites' dielectric permittivity even with low concentration[11,31-33]. In this letter, we propose a way to improve the dielectric permittivity of PI while maintaining low loss tangent. Surface functionalized CCTO nanoparticles with Ag coating are used as fillers. The ultra low dielectric loss of PI makes it most suitable for being as a polymer matrix to process the potential polymer/ceramic composite[34].

Experimental:

CCTO nanoparticles were prepared by the precursor oxalate route[35]. The deposition of Ag nanoparticles on CCTO surface was performed by a modified seeding method[36]. $SnCl_2$ (anhydrous), $AgNO_3$, sodium hydroxide (NaOH) and NH_4OH were purchased from Sinopharm Chemical Reagent Co.,Ltd and used as received. 0.1g of CCTO spheres was dispersed by ultrasonic wave for 30 min in a 50ml water solution of 2% sodium hydroxide. Then pretreated CCTO nanoparticles were added into a 50ml mixed solution of $SnCl_2$ (0.053M) and HCl (0.01M) to induce the adsorption of Sn^{2+} ions on the surface. The colloid was then rinsed for five times with water and moved into a 50ml high Ag concentration solution of ammoniacal silver nitrate (0.27M) for pre-deposition of sliver nuclei. After 30 min, the above solution was rinsed and added into low silver concentration liquor of 2ml ethanol solution of formaldehyde (0.025M), 2ml aqueous solution of animonical silver nitrate (0.05M) and 10ml ethanol. The mixture was airproofed and kept shaking for 17 h while the silver nanoparticles gradually grew uniformly and connected each other (Fig.1).

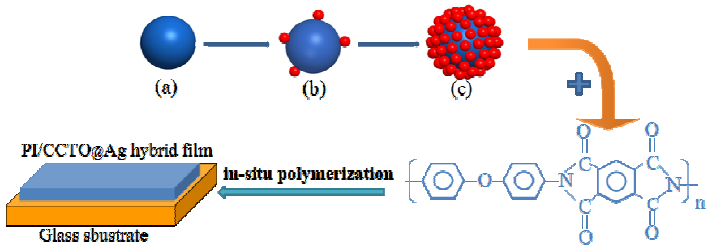

Fig. 1 Schemetic images of in-situ polymerization process and the resulted spheres during different coating steps: (a) original CCTO spheres, (b) reduced silver nuclei (red spheres) on the surface and (c) formed silver layer with dense and uniform structure.

PI/CCTO@Ag hybrid films were prepared by in-situ polymerization. A required amount of CCTO@Ag powder, 4-4'-diaminodiphenyl ether (ODA), and N,N'-dimethylacetamide (DMAc) were placed in a clean three-necked round-bottom flask, followed by ultrasonication for 30min. The ODA was then dissolved in DMAc and a uniform suspension was formed. Afterwards, pyromellitic dianhydride (PMDA) was added to the system, and the mixture was stirred for 4h at room temperature. Subsequently, the mixture was cast onto a piece of clean glass plate, and thermally imidized at 60, 100, 200, and 300 ℃for 1h, respectively. As a result, brown PI/ CCTO@Ag hybrid films with thicknesses of 40μm were obtained. X-ray diffraction (XRD) measurements were carried out by using a D8 diffractometer. The microstructure of CCTO nanoparticles and fractured cross-surface morphology of the composites were examined by

scanning electron microscopy (SEM, HITACHI S-4800) and Transmission electron microscope (TEM, JEM-2010). The dielectric properties were measured using a precise impedance analyzer (Agilent 4294A) at room temperature in the frequency range from 100 Hz to 1 MHz.

Results and Discussion:

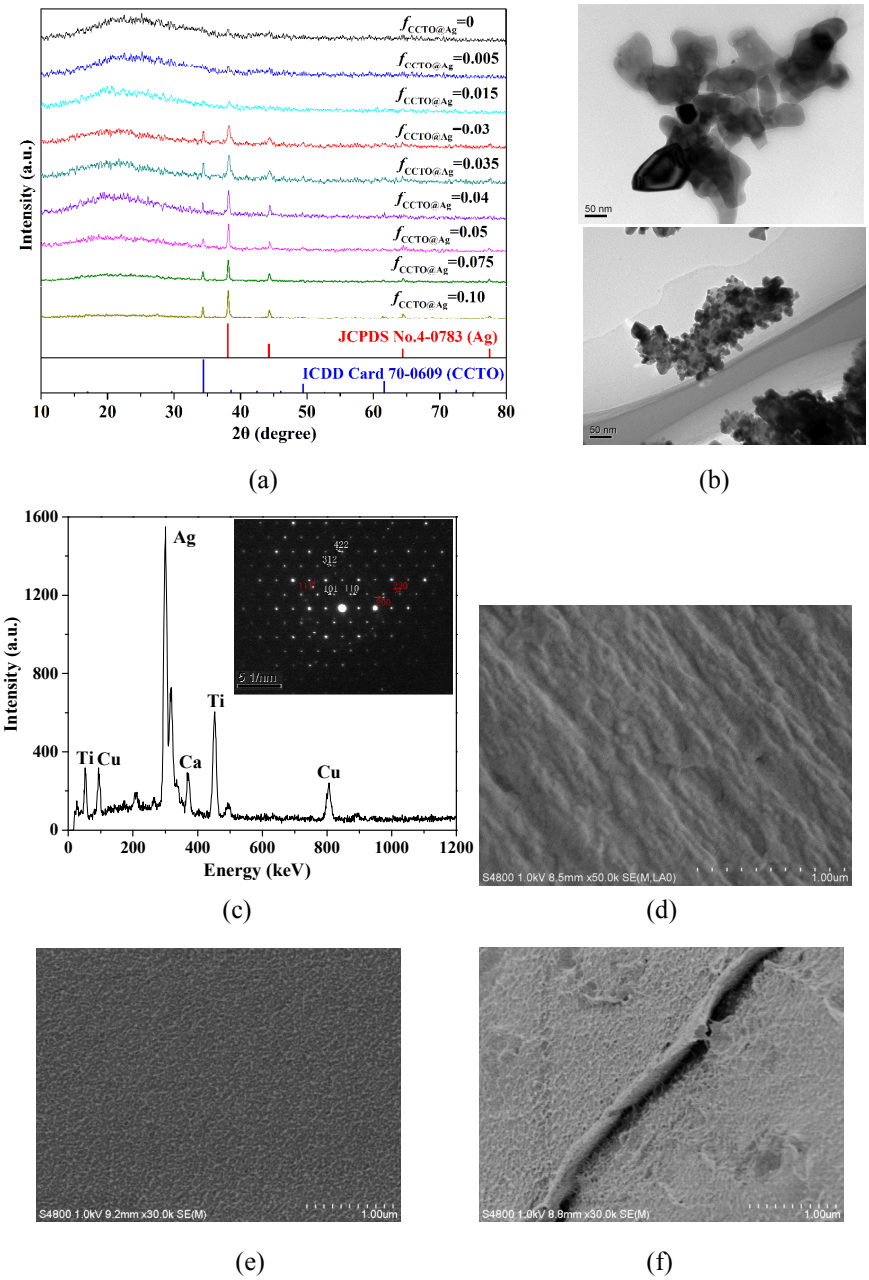

Fig. 2 XRD pattern of PI/CCTO@Ag hybrid films(a); TEM images of CCTO(b up) and CCTO@Ag (b down); EDX analysis of CCTO@Ag (inner part: diffraction pattern (white for CCTO and red for Ag)(c); SEM morphology of the fractured cross-surface of (d) pure PI, (e) PI/CCTO@Ag (3vol%) hybrid film, (f) PI/CCTO@Ag (10vol%) hybrid film.

The X-ray diffraction patterns of pure PI, PI/CCTO@Ag nanocomposites are shown in Fig. 2a. The results of hybrid films show four well defined strong peaks at 2θ =38.1°, 44.3°, 64.5° and 77.6°, corresponding to (111), (200), (220) and (311) planes of the face-centered cubic (fcc) Ag phase (JCPDS No.4-0783), respectively. The diameter of Ag nanoparticles on the surface is estimated to be 36nm using Scherrer equation: d=kλ/(βcosθ) (Where 2θ is the diffraction angle, k is a constant of 0.9, β is the full width at half-maximum of the reflection peak and λ is the X-ray wavelength). The positions and relative intensities of diffraction peaks of CCTO nanoparticles are in good agreement with the Portable Document Format (PDF) card of CCTO from International Center for Diffraction Data (ICDD card 70-0609), and no impurity phase is detective[31,37]. The images in Fig. 2 b show that CCTO is in non-spherical shape and well faceted with an average diameter of 80nm. The bright field image indicates CCTO is uniformly coated with Ag particles. The diameter of Ag particle is estimated to be 36nm, which agrees well with XRD results. The diameter of CCTO particle is estimated to be 36nm, which agrees well with XRD results. Besides Ca, Cu and Ti peaks resulting from CCTO particles, only Ag peak could be found in the pattern (Fig.2c). Together with the combination of diffraction pattern in Fig. 2c, this means Ag coating layer with high purity is obtained. The images of fractured cross-surface in Fig.2 d-f show that when the concentration is low, CCTO@Ag is homogeneously dispersed in PI matrix to form a random composite. At high filler loading, the voiding (porosity) occurs due to the agglomeration and imperfect packing of fillers and the solvent evaporation.

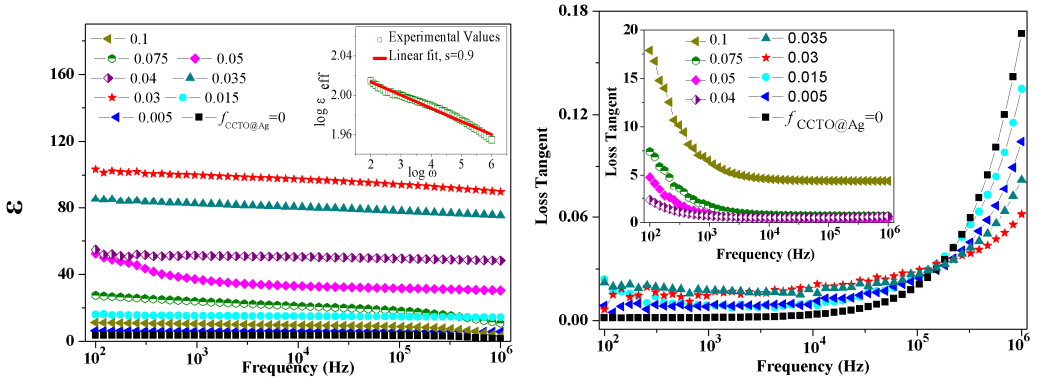

(a) (b)

Fig. 3. Dependence of dielectric permittivity (ε) and loss tangent on frequency of PI/CCTO@Ag hybrid films with different $f_{CCTO@Ag}$ at room temperature (the scatter symbols in b represent the same filler loading in a).

Fig. 3 shows the dependence of dielectric permittivity (ε) (a) and loss tangent (tanδ) (b) on

frequency with different volume fractions in the frequency range of 100Hz-1MHz at room temperature. It is found that both ε and tanδ increase gradually with filler content. The hybrid film has largest dielectric permittivity of 103 (100Hz) when the content of CCTO@Ag is 3vol%. Dielectric loss keeps at a low level (0.018 at 100Hz) at the same loading (Fig.3b). In comparison with pure PI (ε=3.5), dielectric permittivity of the composite is nearly 30 times higher. It is shown that the incorporation of conducting fillers in polymer matrix will result in the increase of dielectric permittivity[38]. Besides, the remarkable enhancement of dielectric permittivity is attributed to the enhancement of Maxwell-Wagner-Sillars (MWs) effect[39]. That is, the increment of conductivity of the interlayer between CCTO and PI by Ag enhances the space charge polarization and MWs effect, which play a very important role in improving the dielectric permittivity [40,41]. Thus, owing to the MWs effect, lots of charges are blocked at the interfaces between the filler and polymer matrix, which makes a remarkable contribution to the increment of the dielectric permittivity.

To estimate the effect of interfacial polarization, we fit the dielectric constant and frequency to eq. $\varepsilon_{eff} \propto \omega^{u-1}$, where ω is the angular frequency (equal to $2\pi f$) and u is a critical exponent, always between 0 and 1. Fitting the dielectric constant data of three-phase composites with $f_{Graphene}$=3.2vol%, yields u=0.9 (Fig.3a inset). This value is in neighborhood of the theoretical value u=0.7 predicated by the percolation theory, indicating the effective influence of space charge polarization on the dielectric response in the composites. That is to say, the MWs polarization plays a significant role in obtaining high ε_{eff} as more interfaces are introduced after the third phase of Ag on the surface of CCTO, especially when the filler contention approaches to the percolation threshold. The drop of the dielectric permittivity at high filler loading is attributed to the agglomeration of the filler in polymer matrix(Fig 2f). It can be observed that there is a frequency dependence of dielectric permittivity as well as dielectric loss in all of these composites. At high frequency, the dipole fails to respond rapidly to follow the change of field and dipole polarization decreases, so the dielectric permittivity tends to decrease.

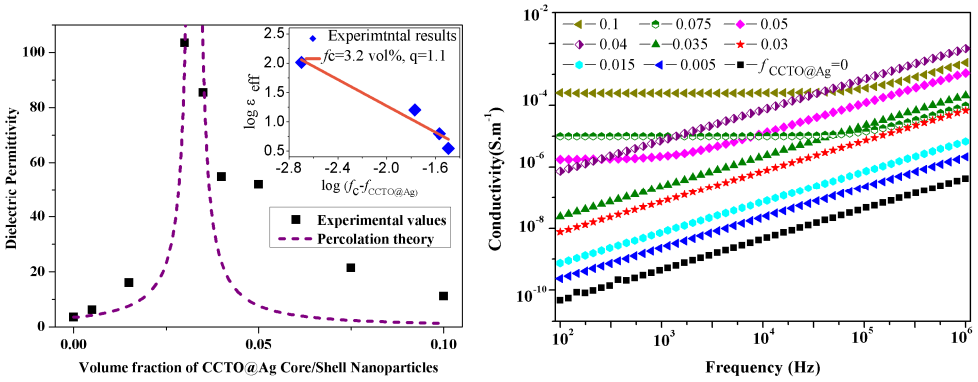

(a) (b)

Fig.4 Comparison of experimental and theoretical dielectric permittivities of PI/CCTO@Ag nanocomposites as a function of volume fraction of CCTO@Ag fillers at 100Hz and room temperature(a); Dependence of AC conductivity of PI/CCTO@Ag composites on frequency (b).

To clarify the mechanisms of the composites' dielectric properties, the percolation theory is put forward to predict the dielectric permittivity of the composite at 100Hz and room temperature. The variation of the dielectric permittivity in the neighborhood of the percolation threshold is given by the power law, $\varepsilon = \varepsilon_1 \left| \left(f_c - f \right) / f_c \right|^{-q}$ (where ε_1 is the dielectric permittivity of polyimide, f is the volume fraction of filler, f_c is the percolation threshold)[42]. Fig. 4a shows that experimental results fit well with percolation theory when f is below the percolation threshold (the fitting parameter f_c and q are 3.2vol% and 1.1, respectively). The linear fit of the log value dielectric permittivity and volume fraction also indicates the dielectric property fit well with the percolation theory below the percolation threshold (Fig 4a inset)[42]. The universal values of percolation threshold f_c and critical exponent q are f_c ~16%-20%, q~0.8-1 for two-phase random media. The critical exponent is a normal value and the decrease of percolation threshold is attributed to the conductive Ag particles on the surface[42]. These researches indicate that the properties of polymer nanocomposites are not only determined by the raw fillers but also should be ascribed to the process conditions and physicochemical characteristics of the nanocomposites[41-44]. The understanding of these results could help us to choose proper process conditions and modifications approaches of the raw fillers to obtain desired properties.

In order to present the proof of the low value of percolation threshold, AC conductivity of pure PI and PI/CCTO$_{@}$Ag composites with different concentrations of filler are presented in Fig.4b. It can be observed that the value of conductivity slowly increases for PI/CCTO$_{@}$Ag composites when $f_{CCTO@Ag}$< 3vol%. As further increasing the filler to 4 vol% (higher than the

percolation threshold), an obvious insulator-semiconductor transition is observed, which indicates the formation of conductive paths in the composite. This is attributed to the Ag nanoparticles on the surface that promote the charge transfer. The low filler content at percolation threshold is quite important for the homogenesity of PI/CCTO@Ag composites.

The energy loss due to consumption of a dielectric material can be determined by the following equation: $W = \pi\varepsilon\xi^2 f \tan\delta$, where ξ is the electric field strength and f is the frequency. In order to reduce energy loss, a low loss tangent is preferred especially at high frequency in high energy devices[27]. The loss tangent measured at a certain frequency includes polarization loss and conduction loss. The conduction loss is caused by the charge flow through the composites which depends on the electric conductivity of composites. It can be seen from Fig.4b that the conductivity of filler loading below 3vol% keeps at low level, thus the polarization loss plays the dominant role in these composites. The absorbed insulating polymer chains can act as the dielectric barrier governing the tunneling conduction and make it impossible for complete contacts to be realized between nanoparticle clusters [41,45,46]. At higher filler loading(>4vol%), the sharp increase of dielectric loss (Fig.3b) is ascribed to the conduction loss which is attributed to the high conductivity (Fig 4b). Thus, conduction loss plays the dominate role in the loss tangent at high filler loading [46].

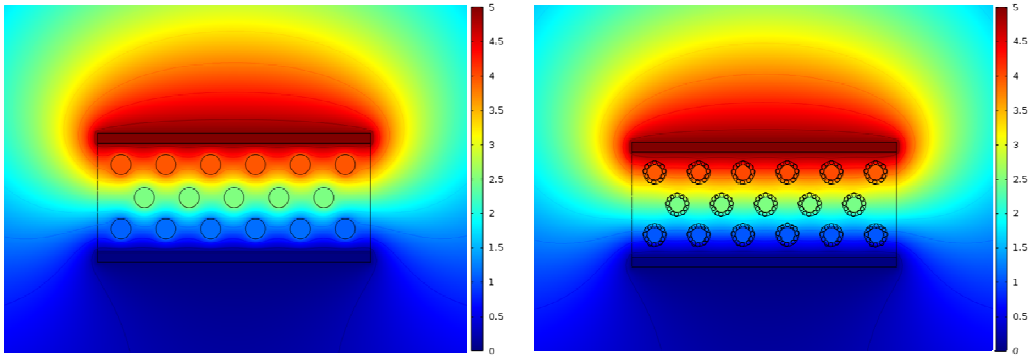

(a) (b)

Fig.5. The outline contours of electrical potential in different materials: a) PI/CCTO(3vol%); b) PI/CCTO@Ag (3vol%, with Ag nanoparticles (diameter: 36nm) on the surface of CCTO). This simulation is done in a capacitor with two parallel platelike electrodes and a dielectric polymer nanocomposite filled with spherical ceramic CCTO nanoparticles (the circles between the two electrodes) and CCTO nanoparticles coating with Ag, the unit of voltage is V.

Dang reported that the homogeneity is mainly determined by the difference of dielectric permittivity of two phases[12]. In order to find the degree of dielectric homogeneity of our

composites, we numerically simulate the electric field distortion in PI/CCTO and PI/CCTO@Ag composites using Comsol Multiphysics. The results show that when embedding CCTO nanoparticles (d=80nm) in polyimide matrix, these particles with high permittivity act as electrical defect centers. Such defect centers effectively distort the distribution of electric field and make the local electric field in the matrix much higher than the average one (Fig.5a). The main drawback of this is that effective permittivity in these composite comes from the increase in the average field of the polymer matrix which is not beneficial to the enhancement of the dielectric permittivity[47,48]. Also the electric field distortion will promote the charge transfer between fillers. By decorating the surface of CCTO nanoparticles with Ag coating, the electric field distortion is much improved (Fig.5b). This implies that the effective permittivity in these composites comes from the increase in average field of both polymer matrix and ceramic filler. The improvement of electric field distortion will make the dipoles better aligned along the field direction and so that the interfacial polarization can be enhanced and the dielectric permittivity can be increased. Besides, charge transfer is suppressed by the insulating polymer matrix leading to low dielectric loss.

The inclusion of CCTO nanoparticles not only leads to high dielectric permittivity in composite due to the large permittivity of particles and MWs polarization but also results in high dielectric loss due to the pores and electric field distortion [21,49,50]. In comparison, by decorating the surface of CCTO nanoparticles with Ag coating, the remarkable enhancement of dielectric permittivity is achieved by the enhancement of MWs effect. Moreover, we have proved that although the Ag particles on the surface of CCTO are conductor, the low loss (0.018 at 100Hz) is achieved attributed to the improvement of electric distortion and blockage of charge transfer by insulating polyimide chains. Low percolation threshold leads to good mechanical properties and material processibility. The easy processibility, good flexibility, and excellent dielectric behavior make PI/CCTO@Ag composites attractive as potential candidates for practical applications in high charge-storage capacitors and embedded devices in electronic industry.

The authors would like to acknowledge the financial support from 973 Program (No. 2012CB821404), Chinese National Foundation of Natural Science (Nos. 51172166 and 61106005), National Science Fund for Talent Training in Basic Science (No. J1210061), Doctoral Programme Foundation (No.20130141110054) and Fundamental Research Funds for the Central Universities (No. 2012202020201).

REFERENCES:

1. Q.M. Zhang, H. Li, M. Poh and C. Huang, *Nature*. 2002, **419**, 284-287.
2. M. Arbatti, X.B.Shan and Z.Y. Cheng, *Adv. Mater.* 2007, **19**, 1369-1372.
3. Y.Zhang, Y. Wang, M. Li and J. Bai, *ACS Appl. Mater. Interfaces.* 2012, **4**, 65-68.
4. J.M.P. Alaboson, Q.H. Wang, J.D. Emery and M.C. Hersam, *ACS Nano*. 2011, **5**, 5223-5232.
5. Y.Shen, Y. Lin, M. Li and C.W. Nan, *Adv. Mater.* 2007, **19**, 1418-1422.
6. C.Huang, Q.M. Zhang and J. Su, *Appl. Phys. Lett.* 2003, **82**, 3502-3504.
7. K. Deshmukh and G.M. Joshi, *RSC. Adv.*, 2014, **4**, 37954-37963.
8. R. Ulrich, *IEEE Trans. Adv. Packag.* 2004, **27**, 326-331.
9. Z.M. Dang, Y.Q. Lin and H.P. Xu, *Adv. Funct. Mater.* 2008, **18**, 1509-1517.
10. Z. M. Dang, H.Y.Wang and H.P. Xu, *Appl. Phys. Lett.* 2006, **89**, 112902**.**
11. W.H. Yang, S.H. Yu and R. Sun, *Acta. Mater.* 2011, **59**, 5593-5602.
12. Z.M. Dang, Y.J. Kai, S.H. Yao and R.J. Liao, *Adv. Mater.* 2013, **25**, 6334-6365.
13. J.X. Lu, K.S.Moon and C.P.Wong, *J. Mater. Chem.*2008, **18**, 4821-4826.
14. Z.M.Dang, Y.Shen and C.W.Nan, *Appl. Phys. Lett.* 2002, **81**, 4814–4816.
15. H.W.Choi, Y.W.Heo, J.H. Lee and J.J. Kim, *Appl. Phys. Lett.* 2006, **89**, 132910.
16. J. Xu, M. Wong and C.P. Wong,*Proceedings of the 54th IEEE Electronic Components and Technology Conference*. 2004, **1**, 536–541.
17. I.R. Abothu, P.M.Raj, D. Balaraman and V.Govind, *Proceedings of the 54th IEEE Electronic Components and Technology Conference*. 2004, **2**, 514–520.
18. J.X. Lu, K.S. Moon, J.W. Xu and C.P. Wong, *J. Mater. Chem.* 2006, **16**, 1543–1548.
19. Y.J.Li, M.Xu, J.Q. Feng and Z.M. Dang, *Appl. Phys. Lett.* 2006, **89**, 072902.
20. Y.Shen, Y.H. Lin and C.W. Nan, *Adv. Funct. Mater.* 2007, **17**, 2405-2410.
21. L. Qi, B.I. Lee, S. Chen and W.D. Samuels, *Adv. Mater.* 2005, **17**, 1777-1781.
22. S.H.Yao, Z.M.Dang, M.J. Jiang and J.BS. Luo, S. Yu, R. Sun and C.P. Wong, *ACS Appl. Mater. Interfaces.* 2011, **6**, 176-182.. Bai, *Appl. Phys. Lett.* 2008, **93**, 182905.
23. Y.Li, X.Y.Huang, Z.W.Hu and P.K. Jiang, *ACS Appl. Mater. Interfaces.* 2011, **3**, 4396-4403.
24. G.S. Wang, *ACS Appl. Mater. Interfaces.* 2010, **2**, 1290-1293.
25. T.Zhou, J.W. Zha, R.Y. Cui and B.H. Fan, *ACS Appl. Mater. Interfaces.* 2011, **3**, 2184-2188.
26. K.C.Li, H. Wang, F.Xiang and W.H. Liu, *Appl. Phys. Lett.* 2009, **95**, 202904.
27. S. Luo, S. Yu, R. Sun and C.P. Wong, *ACS Appl. Mater. Interfaces.* 2011,**6**,176-182
28. L. Xie, X. Huang, B.W. Li, C. Zhi, T. Tanka and P. Jiang, Phys. Chem. Chem. Phys, 2013, 15, 17560-17569.
29. J.Wu, C.W.Nan, Y.H. Lin and Y. Deng, *Phys. Rev. Lett.* 2002, **89**, 217601.
30. C.C. Homes, T.Vogt, S.M.Shapiro and A.P. Ramirez, *Science* 2001, **293**, 673-676.
31. Z.M.Dang, T. Zhou, S.H.Yao and J.B. Bai, *Adv. Mater.* 2009, **21**, 2077-2082.
32. Y.Yang, B.P.Zhu, R.Xiong and J.Shi, *Appl. Phys. Lett.* 2013, **102**, 042904.
33. Y.Yang, R.Xiong, J. Shi and Z.Y.Liu, *APL Materials.* 2013, **1**, 050701.
34. J.A.Kreuz, and J.R.Edman, *Adv. Mater.* 1998, **10**, 1229-1232.
35. P.Thomas, K. Dwarakanatha, K.B.R. Varmab and T.R.N. Kutty, *J. Phys. Chem. Solids.* 2008, **69**, 2594-2604.
36. Y.Kobayashi, V.S. Maceira and L.L. Marzan. *Chem. Mater.* 2001, **13**, 1630-1633.

37. A.P. Ramireza, M.A. Subramanianb, M Gardela, and S.M Shapiroet, *Solid. State. Commun.* 2000, **115**, 217-220.
38. R.W.Sillars, J. Inst. Elec. Engrs., 1937, **80**, 139-155.
39. C.W. Nan, Y. Shen and J. Ma, Annu. Rev. Mater. Res.2010, 40, 131-151.
40. M.Panda, V. Srinivas1, and A. K. Thakuret, *Appl. Phys. Lett.* 2008, **93**, 242908.
41. X.Y. Huang, P.K. Jiang and L.Y. Xie, *Appl. Phys. Lett.* 2009, **95**, 242901.
42. C.W.Nan, *Prog. Mater.Sci.* 1993, **37**, 1-116.
43. X.Y.Huang, C.Kim, P.K. Jiang and Z.Li, *J. Appl. Phys.* 2009, **105**, 014105.
44. L.F.Hakim, J.F. Portman, M.D. Casper and A.W.Weimer, *Powder Technol.* 2005, **160**, 149-160.
45. J. Park and W. Lu, *Appl. Phys. Lett.* 2007, **91**, 053113.
46. I.Balberg, D. Azulay, D. Toker and O. Millo, *Int.J.Mod.Phys.B*. 2004, **18**, 2091-2121.
47. L.An, S.A. Boggs and J.P. Calame, *IEEE Electr. Insul. Magn.* 2008, **24**, 5-10.
48. J.Y.Li, L. Zhang and S. Ducharme, *Appl. Phys. Lett.* 2007, **90**, 132901.
49. H.Stoyanov, D.M.Carthy, M.Kollosche and G. Kofod, *Appl. Phys. Lett.* 2009, **94**, 232905.
50. C.Huang,and Q. Zhang, *Adv. Funct. Mater.* 2004, **14**, 501-506.